INSTITUTE OF PHYSICS PUBLISHING JOURNAL OF PHYSICS: CONDENSED MATTER

J. Phys.: Condens. Matter **15** (2003) 321–332 PII: S0953-8984(03)38908-8

Kinetics of the high- to low-density amorphous water transition

M M Koza[1], H Schober[1], H E Fischer[2], T Hansen[1] and F Fujara[3]

[1] Institut Laue-Langevin, F-38042 Grenoble Cedex, France
[2] Laboratoire LURE, F-91898 ORSAY Cedex, France
[3] Fachbereich Physik, Technische Universität Darmstadt, D-64289 Darmstadt, Germany

Received 7 July 2002
Published 13 January 2003
Online at stacks.iop.org/JPhysCM/15/321

Abstract

In situ neutron diffraction experiments have been carried out to study the kinetics of the transformation of high-density amorphous (HDA) water into its low-density amorphous state at temperatures 87 K $\leqslant T \leqslant$ 110 K. It is found that three different stages are comprised in this transformation, namely an annealing process of the high-density matrix followed by a first-order-like transition into a low-density state, which can be further annealed at higher temperatures $T \leqslant$ 127 K. The annealing kinetics of the HDA state follows the logarithm of time as found in other systems showing polyamorphism. According to the theory of transformation by nucleation and growth the apparent first-order transition follows an Avrami–Kolmogorov behaviour. An energy barrier $\Delta E \approx 33$ kJ mol^{-1} is estimated from the temperature dependence of this transition.

1. Introduction

The experimental identification of two distinctly different disordered states of water at low temperatures [1], namely a high-density amorphous (HDA) ($\rho \approx 1.17$ g cm^{-3}, H_2O) and a low-density amorphous (LDA) state ($\rho \approx 0.93$ g cm^{-3}, H_2O), triggered a strong scientific interest in the phenomenon nowadays known as polyamorphism [2–6]. Extensive experimental and computer simulation studies have been performed to shed light onto the properties of the two amorphous states and to give a coherent explanation for their existence.

It has been shown that both amorphous states can be converted into each other either by heating the sample above $T \approx 100$ K at ambient pressure (HDA $\rightarrow$ LDA) or by compressing the sample above $p \approx 10$ kbar at $T < 160$ K (LDA $\rightarrow$ HDA) which gives evidence of a hysteresis behaviour with respect to the control parameters T and p [2, 7–10]. Strong structural and density changes upon compression can also be observed in the liquid state of water [11, 12], the compressed and the uncompressed states often being referred to as high-density and low-density liquid water, respectively. Calorimetric experiments revealed the release of latent heat

at the HDA → LDA transformation [7], indicating a first-order phase transition. The low-density matrix, on the other hand, shows upon heating an onset of an endothermic transition before it recrystallizes exothermally to cubic ice [7, 13–16]. The endothermic transformation has been interpreted as a glass transition of LDA with $T_g \approx 140$ K [7, 13–16], though new ideas favour a $T_g \approx 165$ K [17].

Although the described experimental results on HDA and LDA are compatible with a first-order transition between two supercooled liquid states and experimental results are often referred to as due to a first-order phase transition, so far, there has been no unequivocal evidence given either for a first-order transition line between HDA and LDA or for their relation to liquid states via a glass transition. Moreover, some experimental results oppose the idea of HDA and LDA being supercooled liquids. For example, inelastic neutron and x-ray scattering experiments have revealed a rather harmonic, crystal-like dynamics of HDA and in particular of LDA [18–29].

Three distinct models have been discussed in contemporary literature to account for the existence and the properties of the two amorphous states [30–32]. Apart from the proposed second critical point ($T_c \approx 220$ K, $p_c \approx 1$ kbar) with an emerging line of first-order transition towards lower temperatures [33], a retracing of the vapour–liquid spinodal in the supercooled region of water's phase diagram [34–36] and a singularity-free scenario [37, 38] offer possible explanations for the observed phenomena. Poole *et al* [39] succeeded in introducing a thermodynamic model which shows that the second critical point and the retracing spinodal scenarios are fundamentally related and both incorporate a phase transition between two distinct liquid phases at low temperatures. In contrast to the model of Poole *et al* in which intermediate states of the transition should reflect the superposed properties of the phases involved, the singularity-free model implies a continuous change of observables. The *in situ* sampling of the static structure factor gives us, in principle, the opportunity of extracting information on the kinetics of the transformation and on the properties of the intermediate states, i.e. to distinguish between continuous variation of the amorphous structure and a superposition of the HDA and LDA structures in the course of the transformation.

The paper is structured as follows. We first describe the sample preparation and give some information on the experimental procedure. We then present the experimental results for the three transformation stages and finish with a general conclusion.

2. Experimental methods

All HDA samples were prepared by slow compression of deuterated crystalline ice I_h ($V \approx 2.5$ ml) in a piston–cylinder apparatus at $T = 77$ K up to $p \approx 17$ kbar [40, 41]. After HDA had been formed the pressure was released and the sample retrieved from the pressure device under liquid nitrogen and transferred in cylindrical sample containers into precooled ($T = 77$ K) standard Orange cryostats [42]. The evaporation of nitrogen from the sample containers was carried out at $T = 78$–79 K and controlled via the static structure factor of the samples. Throughout this paper the states which we refer to as HDA and LDA correspond to the amorphous states as obtained by pressure amorphization at $T \approx 77$ K (HDA) and after annealing at $T = 127$ K (LDA). For each sample the static structure factor of HDA and, after the *in situ* measurements, of LDA was determined at $T = 77$ and 127 K, respectively. At these conditions both amorphous states could be well reproduced. The effect of elastic density changes of the sample upon temperature variation has been estimated from measurements of the static structure factor at equal temperature. The error proved to be of the order of 1%, i.e. an order of magnitude smaller than the effects discussed here.

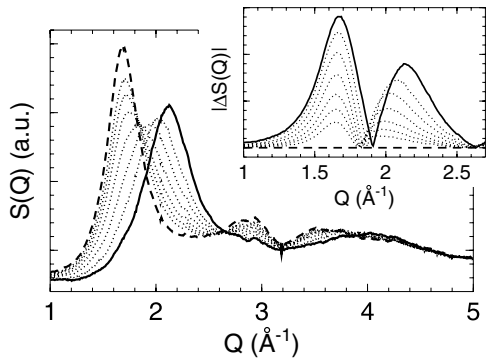

Figure 1. Evolution of the static structure factor $S(Q)$ during the transition from HDA (solid curve) into LDA (dashed curve) water. Intermediate data (dotted curves, maximum shifting from right to left) are selected from an *in situ* measurement of the HDA to LDA transition performed on the diffractometer D20 at ILL. The inset shows the difference of $S(Q;T)$ taken at corresponding conversion stages with respect to $S(Q;\mathrm{LDA})$, the static structure factor of LDA, $|\Delta S(Q)| = |S(Q;\mathrm{LDA}) - S(Q;T)|$.

Two different types of thermal treatment were applied to the samples. First, measurements were performed on samples that were heated directly from the HDA state to the nominal temperature T. A second set of experiments was performed on samples that had been preannealed at a temperature T_{an} and heated subsequently to the nominal T with 77 K $<$ $T_{\mathrm{an}} < T <$ 127 K. The data collection started in all cases before the heat treatment was applied. This allowed us to monitor the transformation process continuously. Data were collected on the diffractometer D4 (incident neutron wavelength $\lambda_{\mathrm{i}} = 0.7$ Å) and D20 ($\lambda_{\mathrm{i}} = 1.3$ and 2.4 Å) and the time-of-flight spectrometer IN6 ($\lambda_{\mathrm{i}} = 4.1$ Å) at the Institut Laue Langevin in Grenoble, France [42]. Detailed information on the applied temperatures, the instruments used for different measurements and the data acquisition time are given below and can be retrieved from the presented figures.

The raw data are corrected for different detector efficiencies and for empty container scattering. To compare the energy-resolved time-of-flight data (IN6) with those from the diffraction instruments (D4 and D20) an energy integration is performed as $S(2\Theta) = S(2\Theta, t = 0) = \int S(2\Theta, \omega)\,\mathrm{d}\omega$. All data sets are finally converted onto Q-space via the mapping $S(2\Theta) \rightarrow S(Q)$. Figure 1 shows the obtained $S(Q)$ of HDA and LDA as measured on D20. For the discussion of the kinetics data are taken into consideration which have been obtained when the sample temperature has arrived within an offset of 2 K from T.

3. Results and discussion

To quantify the HDA to LDA transition we need to define an order parameter indicating the relative proximity of a given atomic structure to that of the initial HDA or the final LDA. An obvious choice is the atomic number density, which can differ by more than 20% between HDA and LDA. The irregular granular nature of our samples made an accurate determination of the sample volume illuminated by the neutron beam impossible, so we can only parametrize relative changes in density. A Fourier transform of $[S(Q) - 1]$ gives directly a pair-correlation function $G(r)$ having a line at small r whose slope is proportional to the atomic number density. However, the maximum Q in our diffractograms (D4, 17 Å^{-1}; D20, 9 Å^{-1}; IN6, 2.7 Å^{-1}) was not sufficient to give the needed r-space resolution even for relative changes in the slope of the density line in $G(r)$.

On the other hand, as shown in [11] the position of the maximum in $S(Q)$ scales approximately with the density of an amorphous water sample. It may therefore be expected to reflect the density change as a characteristic order parameter. However, the statistical quality of the evaluated peak position depends strongly on the experimental conditions, which influence the Q-resolution and the statistics of the data. For this reason accurate information on the kinetics of the HDA to LDA transformation can not be extracted from all present data sets.

Our scientific interest in this paper primarily concerns the HDA $\rightarrow$ LDA transition itself. We, therefore, refrain from an absolute interpretation of the measured structure factors and instead base our analysis on the relative changes observed while the sample passes from the HDA into the LDA state. A convenient mathematical expression for monitoring these changes is provided by the difference profile obtained from subsequent data sets with respect to a reference $S(Q)$, e.g. the $S(Q)$ of LDA [26].

More specifically, we map the diffractograms onto the space of positive real numbers via the integral

$$I(t, T) = \int_{Q_1}^{Q_2} |S(Q; \mathrm{LDA}) - S(Q; t, T)| \mathrm{d}Q \Big/ \int_{Q_1}^{Q_2} |S(Q; \mathrm{LDA}) - S(Q; \mathrm{HDA})| \, \mathrm{d}Q. \quad (1)$$

$S(Q; \mathrm{HDA})$ and $S(Q; \mathrm{LDA})$ denote the static structure factors of HDA and LDA determined at $T = 77$ and 127 K, respectively. According to the above definition $I(t, T)$ is taking on the values one for HDA and zero for LDA. The rather heuristic quantification of the kinetics via equation (1) has the advantages of mathematical simplicity and a certain impartiality towards any particular features in $S(Q)$.

In a pure first-order transition the structure factors of the intermediate states can be expressed as a superposition of those of the initial and final phases. In that case $I(t, T)$ would simply represent the fraction of initial material, in our case HDA, still present in the sample at time t and temperature T.

An example for the integrand $|\Delta S(Q)| = |S(Q; \mathrm{LDA}) - S(Q; t, T)|$, which corresponds to the absolute value of the difference profiles, is shown in the inset of figure 1. From a purely mathematical point of view we can choose the integration limits arbitrarily. Results are physically relevant only if they do not depend on the integration limits. For practical reasons we chose $Q_1 = 1$ Å^{-1} and $Q_2 = 2.65$ Å^{-1}. This range is covered by all our experiments and thus makes it possible to compare all data sets consistently. In addition the difference profile $|\Delta S(Q)|$ is approximately zero at these Q-values. The main conclusions of our analysis are completely independent of this choice as demonstrated by the fact that they can e.g. equally be obtained by concentrating solely on the first peak of the static structure factor. A comparison between $I(t, T)$ as it is obtained from equation (1) and from the position of the first peak in $S(Q)$ is presented in figure 2. Beyond the qualitative differences between the two data sets, the inflection point of both curves, which will be taken later on in this paper for a measure of the transition time constant, is the same in both cases. This is best emphasized by the transition rate $\mathrm{d}I(t, T)/\mathrm{d}t$ presented in the inset of figure 2. The difference between the two presented curves is based on the fact that results from equation (1) are sensitive not only to shifts of the peak in $S(Q)$ but also, for example, to variation of its width. Thus, in a simplified manner, we may expect the peak position to reflect the progressive rearrangement of water molecules into a tetrahedrally coordinated network as outlined in reference [43]. Equation (1) may account in addition for variation of the correlation length, i.e. in the case of LDA for the reorientation of single tetrahedra in respect to each other. In particular, the final stages of the conversion into LDA are characterized by a narrowing of the first structure factor maximum rather than a shift of its maximum as can be judged from figure 1. This behaviour indicates a progressive increase of the correlation length.

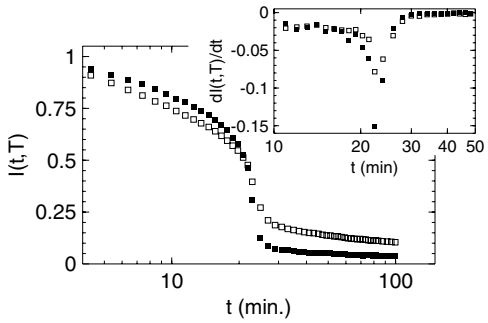

Figure 2. Comparison of $I(t, T)$ extracted from the position of the peak in $S(Q)$ (black squares) and from the evolution of $S(Q)$ given by equation (1) (open squares). The inset displays the transition rate $\mathrm{d}I(t, T)/\mathrm{d}t$. Please note that both techniques of calculating the transition kinetics give identical values for the $\mathrm{d}I(t, T)/\mathrm{d}t$ minima, which represent the time constant of the transition.

All $I(t, T)$ as extracted with equation (1) from our data are presented in figures 3 and 4 as a function of time for various temperatures. Figure 3 displays data obtained on samples having been heated directly from the HDA state to the nominal temperatures. Throughout all measurements at $T \leqslant 97$ K the monitored kinetics follows a logarithmic dependence on t which is emphasized by the logarithmic abscissa. At temperatures $98 \leqslant T \leqslant 100$ K the onset of a second process is announced by a kink in $I(t, T)$. At higher temperatures $I(t, T)$ transforms into a sigmoid-shaped curve whose inflection point is shifted to earlier time t as T increases.

Transformation kinetics of samples which have undergone annealing are shown in figure 4. As in the unannealed case, data taken at 97 K show a pronounced logarithmic behaviour. For temperatures above 103 K a characteristic sigmoidal dependence on time is observed.

Among the different functions which have been engaged to account analytically for the time dependence of $I(t, T)$ [26] the best fit is offered with a superposition of a logarithmic response and an Avrami–Kolmogorov equation (AKE) [44]

$$I(t, T) = (1 - C) + C \exp[-(t/\tau_0(T))^n] + B \ln(t). \tag{2}$$

Throughout all fits equation (2) proves to be accurate in describing the time evolution of the data up to 105 K. Its failure at $T = 110$ K is attributed to the rapid heat release at this temperature which cannot be evacuated properly by the sample environment resulting probably in a loosely defined temperature [7]. For low temperatures ($T < 98$ K) the parameter C can be set to zero as stressed by the straight solid lines in figure 3 at $T \leqslant 98$ K and in figure 4 at $T = 97$ K. Physically this result implies that the timescale $\tau_0(T)$ associated with the AKE contribution $I(t, T) \sim \exp[-(t/\tau_0(T))^n]$ exceeds appreciably the experimental time window, leaving a uniquely logarithmic time dependence which is to be attributed to the relaxation of the high-density phase.

For those data sets which allow a reliable fit of the exponential part of function (2) we find that the parameter C covers values between 0.4 and 0.5. While it is not possible to establish a systematic dependence of C on T, the parameter B increases monotonically as T increases, which can be extracted from all fits performed with $C = 0$ in figure 3.

Concerning the logarithmic part of equation (2) a similar dependence—albeit for other sample properties—has been observed in other amorphous materials. Primak [45] and Karpov and Grimsditch [46] show that the density of vitreous silica changes upon heating according to the logarithm of time. During compression of the polyamorphous systems SiO_2 and GeO_2

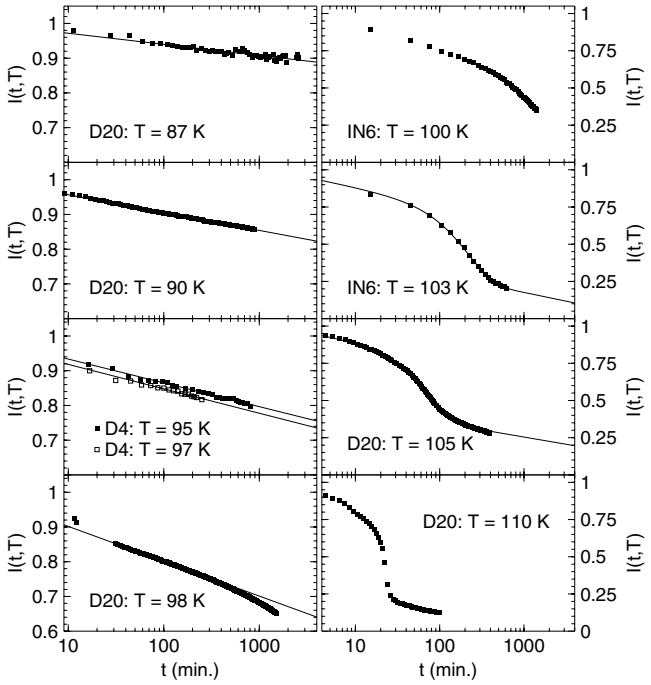

Figure 3. Temperature dependence of the transformation kinetics of HDA to LDA. The definition of $I(t, T)$ is given in the text; the temperatures and instruments are given in the figure. Solid lines in the left-hand column of the figure stress the logarithmic time behaviour of the transition at low temperatures, which give evidence of an annealing of the HDA matrix. The sigmoid-shaped dependence of $I(t, T)$ can be analytically represented by a superposition of the logarithmic HDA annealing and an Avrami–Kolmogorov behaviour, reminiscent of a first-order transition. Such fits to the data correspond to the sigmoid-shaped solid lines on the right-hand side of the figure.

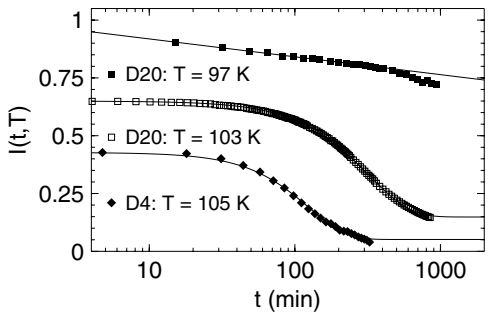

Figure 4. Temperature dependence of the transformation kinetics of HDA to LDA after annealing of HDA at different temperatures T_{an}. T_{an} was chosen as 87 K (black squares), 98 K (open squares) and 101 K (black diamonds). A detailed description of the annealing procedure is given in the text. The nominal temperatures T are shown in the figure. Black diamond data are shifted by 0.15 toward lower values. Solid lines represent fits with ln (t) to black squares and with a pure AKE to open squares and black diamonds.

Grimsditch [47] and Tsiok *et al* [48] demonstrate that changes in the velocity of sound and density scale with the logarithm of time. From a theoretical point of view a logarithmic response $I(t, T) \sim \ln(t)$ is expected for the relaxation of a material possessing a uniform distribution of double-well potentials. The existence of such double wells in amorphous material has been

suggested from their low-temperature properties [46]. Beyond the experimental results recent computer simulations on simple liquids show clearly that experimental observables follow a logarithmic behaviour when aging effects are considered [49].

However, none of these experiments reveal any additional transformation stages beyond the logarithmic relaxation. The applicability of an AKE above some 103 K constitutes strong evidence for an additional transformation process consistent with a first-order transition, i.e. the nucleation and growth of a homogeneous low-density phase within a homogeneous high-density matrix. $\tau_0(T)$ is the temperature dependent time constant governing this transformation. The exponent n is a characteristic parameter of the transformation which is determined by the geometry of the growing particles, the nucleation time constant and the kinetic constraints. For diffusion controlled transitions with short nucleation times and isotropic growth we expect $n = 1.5$ [44]. The exponent n of the AKE shown in figures 3 and 4 spans the interval of 1.5–1.6. Setting n to the constant value of 1.5 neither alters the other parameters markedly nor influences the quality of the fits. This statement holds independently from the annealing of the sample. In spite of this agreement between the theoretical prediction and the experimental data $n = 1.5$ may not hold for other observables as has been discussed by Hage *et al* [50, 51] on the transformation from hyper-quenched glassy water into the crystalline cubic ice, which we refer to later on. The representation of the kinetics at $T = 110$ K leads to elevated n values which can be seen from the sharper transition in figure 3. In this case, n has been estimated as 3.5–4 by best fits to the data.

The two-stage transformation scenario emanating from our data analysis agrees with the differential calorimetry results of Handa *et al* [7]. The latter equally show that the HDA $\rightarrow$ LDA transition comprises at least two conversion steps, namely an annealing of HDA and a subsequent transition of apparent first order to LDA. Assuming that a perfectly annealed HDA state exists and that it can be accessed by proper thermal treatment of the sample we may expect that it shows transformation kinetics following a pure AKE dependence upon further heating. Accordingly, fits ($B = 0$ in equation (2)) to the data taken at $T = 103$ and 105 K on preannealed samples are presented in figure 4 as solid lines. Data at $T = 97$ K are taken on a sample annealed at 87 K for $t \approx 43$ h (figure 3$T = 87$ K), data at $T = 103$ K are taken on a sample annealed at 98 K for $t \approx 25$ h (figure 3$T = 98$ K) and data at $T = 105$ K are taken on a sample kept at 95 K for $t \approx 6.5$ h, at 98 K for $t \approx 5$ h and at 101 K for $t \approx 5$ h (data are not shown in this paper). The data sets measured at 103 and 105 K are well characterized by a pure Avrami–Kolmogorov behaviour, which indicates that well annealed HDA states can indeed be reached.

The final states after the apparent first-order transition at a given T do not coincide with the LDA state obtained after annealing at $T = 127$ K as can be judged from the kinetics curves in figures 3 and 4 whose $I(t, T)$ do not decrease to zero. This implies that we are dealing with a suite of distinct amorphous states that belong to two separate mega-basins (HDA and LDA) on the energy landscape as proposed in [10, 52]. HDA as formed at $T = 77$ K and LDA as obtained at $T = 127$ K are particular states among others in those mega-basins. We expect, therefore, the parameters C and B to be dependent on T and on the thermal history of the sample, which may be represented by the annealing temperature T_{an}. In principle, the double-well potential model of Karpov and Grimsditch [46] allows us to gain information on the energy landscape of the vitreous system under investigation, but it requires C and B values on an absolute scale. Thus, this model cannot be exploited in detail from the present data.

A good test of the proposed two-stage scenario is the superposition of structure factors. As already mentioned for a first-order transition the intermediate states should be a superposition of the initial and final phases. For the intermediate static structure factor $S_{\mathrm{i}}(Q)$ this means that

$$S_{\mathrm{i}}(Q) = (1 - c)S_{\mathrm{HDA}'}(Q) + cS_{\mathrm{LDA}'}(Q), \tag{3}$$

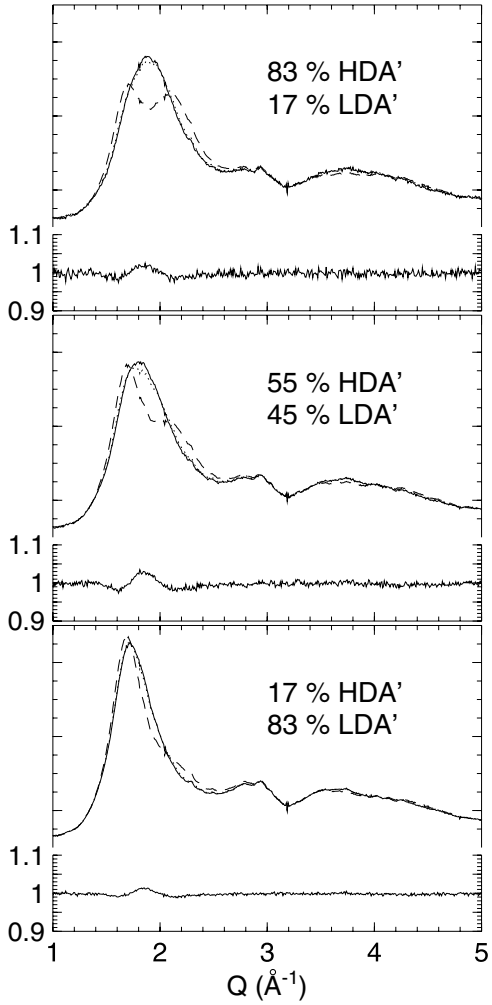

Figure 5. Selected static structure factors $S(Q)$ determined in the course of the HDA $\rightarrow$ LDA transition. Solid curves are intermediate $S(Q)$ measured at $T = 103$ K, dotted curves correspond to best fits superposing the measured initial (HDA′) and final (LDA′) states of the transition at $T = 103$ K (figure 4) and dashed lines represent best fits with a superposition of the HDA and LDA structures as obtained at 77 and 127 K, respectively. The relative contributions to the intermediate $S(Q)$ of HDA′ and LDA′ are given in the figure. Bottom panels in the subfigures display the relative deviations of the fitted HDA′ and LDA′ superposition from the measured intermediate $S(Q)$. The maximum deviations observed are less than 4%.

with c the fraction of the final phase LDA′ in the sample. The primes indicate that we are dealing with the initial annealed HDA and the as-produced LDA at this very temperature. In figure 5 we demonstrate that equation (3) can be well fulfilled at $T = 103$ K with HDA′ representing an annealed ($T_{an} = 98$ K) initial and LDA′ the as-produced LDA state. In contrast we are unable to come up with a superposition of HDA and LDA (annealed at 127 K) reminiscent of the intermediate transition state at 103 K. The structure factors used for the superposition of the intermediate states are shown in figure 6. This result underlines the importance of the relaxation processes both before and after the apparent first-order transformation.

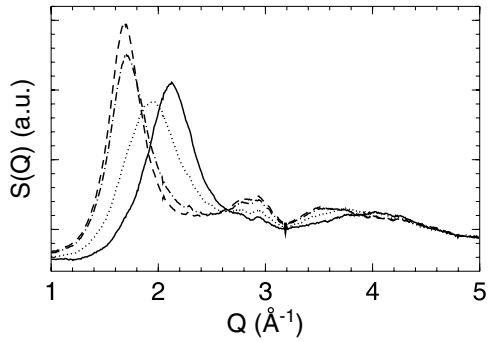

Figure 6. Static structure factor of HDA produced at 77 K (solid curve), LDA obtained at 127 K (dashed curve), HDA′ obtained after annealing at 98 K (dotted curve) and LDA′ obtained after the transition at 103 K (dashed–dotted curve).

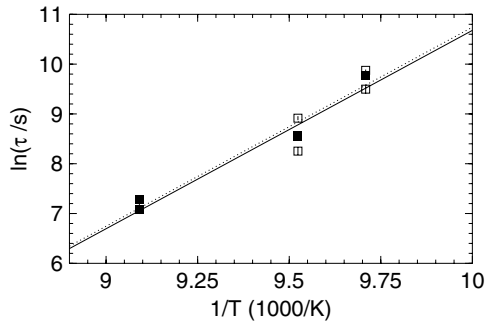

Figure 7. Arrhenius plot of time constants calculated by different techniques—open squares determined with equation (1) and full squares calculated from position of maximum in $S(Q)$. Lines correspond to linear fits, estimating the fit uncertainty by the deviation of all data points (solid line) and by taking the experimental error and temperature step width into account (dashed line).

So far we have not talked about the time constant governing this transition. Since the AKE describes the transition kinetics in an idealized manner we have to be careful when extracting $\tau(T)$ from a simple fit of AKE to the data. In particular the long-time limit of the transition when growing domains interfere with each other is not correctly described by the equation. We therefore estimate the significance of the fit by a variation of the long-time fit limits. Another check is provided by the fact that $\tau(T)$ as extracted from the fit should be directly related to the maximum of the numeric derivative $\mathrm{d}I(t, T)/\mathrm{d}t$ via $t_{\max} = (\frac{n-1}{n})^{\frac{1}{n}}\tau(T)$, as mentioned above and shown in figure 2. Both techniques of extracting $\tau(T)$ have been applied to data obtained by equation (1) and the monitoring of the peak position in $S(Q)$.

Assuming that the transition is based on a thermally activated process the Arrhenius equation

$$\tau(T) = \tau_\infty \exp(\Delta E/RT) \tag{4}$$

can be exploited to determine the activation energy ΔE. The inverse time constant τ_∞^{-1} may be identified with a trial frequency at which the energy landscape is sampled. All calculated $\tau(T)$ are shown in an Arrhenius plot in figure 7.

It is evident from figure 7 that the accuracy of estimating ΔE and τ_∞ is limited rather by the divergence of data extracted by the different techniques than by the experimental errors. Thus,

taking into account the experimental error and the temperature step width, on one hand, and only the divergence of data points on the other gives comparable values of $\Delta E = (33 \pm 2)$ kJ mol^{-1} and $\tau_\infty \approx 10^{-13\pm1}$ s. The value of τ_∞ corresponds to characteristic times of molecular vibrations and librations of solid water phases which extend up to $\hbar\omega \approx 40$ meV and $\hbar\omega \approx 110$ meV, respectively [19, 22, 26]. It represents therefore a physically reasonable attempt time for crossing the energy barrier ΔE.

To stress the significance of ΔE it is to be compared with the energy barrier $\Delta E' = 66 \pm 10$ kJ mol^{-1} (D_2O) found by Hage *et al* [50, 51] for the recrystallization of hyperquenched glassy water (HGW) at $T \approx 150$ K to cubic ice. HGW resembles LDA in structure and density; its recrystallization energy may be taken in good approximation as a reference for the LDA recrystallization properties. As $\Delta E'$ imposes a stability criterion for LDA it places an upper limit on ΔE, which is respected by the value determined from our data. In fact, judging from recent experiments [28], we may expect a slightly elevated value $\Delta E'$ for LDA in comparison to HGW.

4. Conclusions

The present results show clearly that the HDA to LDA transformation incorporates three stages, which may be understood as an annealing of a high-density state, followed by an accelerated transition from the high-density to the low-density modification and ending with an annealing of the low-density matrix. The observed annealing implies that the structures known as HDA and LDA are not well defined. In terms of energy they must be interpreted as loosely defined states in two mega-basins in which they undergo relaxation processes upon temperature and possibly upon pressure changes. Judging from our observations in preceding experiments on the dynamic properties of HDA on D_2O samples [26] we conclude that HDA is not structurally stable at $T = 80$ K, either. Changes in the static structure factor have been detected after six hours of experiment. In fact, on the grounds of a continuous logarithmic annealing process we may expect HDA not to be structurally stable even at lower temperatures and the state known as HDA produced at 77 K not to be an exclusive structure. A variation of the diffraction pattern of HDA as produced at different temperatures ($T \leqslant 140$ K) indicating the variety of HDA states has been also observed by Mishima [10].

The temperature-induced transition from the megabasin of higher density into that of lower density is accomplished by surmounting an energy barrier of about 33 kJ mol^{-1}. Within the accuracy of our data this transition only accounts for about 40–50% of the changes observed in the static structure factor over the full HDA $\rightarrow$ LDA transition. The analytical description of the kinetics in this regime by an AKE and the good agreement of the superposition of the initial and final structures with the measured intermediate static structure factor meets the condition for a first-order transition. It must be emphasized that the intermediate structures do not coincide with a superposition of HDA and LDA structures as produced by compression at 77 K and obtained after the transition at 127 K, respectively. A first-order transition is also in agreement with the observed change of the static structure factor at low Q values [26, 55], which is indicative of a transient contrast increase in the course of the HDA to LDA transformation.

Despite the fact that our data meet the conditions for a first-order transition they do not constitute a definitive proof for this transition scenario. In addition, it has to be pointed out that our results do not imply any connection or relation between the two studied amorphous structures and the liquid phase or the supposed liquid states, either. The outlined first-order transition between HDA and LDA must be understood as a constraint on any theoretical concept which may account for the nature of these amorphous states. However, in consideration of different water models our results strongly support the scenarios introduced by

Poole *et al* [39] including the second-critical-point scenario [33] and the stability limit conjecture [34–36]. The model and explanations given in [39] are tempting since they are able to account for both the liquid behaviour of water and the properties of the amorphous states. On the other hand, our results, in particular the successful superposition of HDA′ and LDA′ structure factors to account for the structure of intermediate states, are not consistent with a singularity free scenario as is outlined in [37, 38]. Although recent diffraction results are interpreted in favour of a continuous conversion of HDA into LDA [56], they are based on experimental conditions within the annealing limits of HDA, as outlined here[4], and contradicted by latest Raman experiments [57].

The implications of this observation are manifold. In particular, the variety of high- and low-density structures must be acknowledged in any attempt at connecting the liquid phase of water with the amorphous solid states by inter- or extrapolating experimental results.

Acknowledgments

We wish to thank Pierre Convert for having granted us access to the high-flux diffractometer D20 at ILL during its commissioning. We also acknowledge the financial support by the German *Bundesministerium für Bildung und Forschung* under project 03Fu4DOR5.

References

[1] Mishima O, Calvert L D and Whalley E 1984 *Nature* **310** 393
[2] Mishima O, Calvert L D and Whalley E 1985 *Nature* **314** 76
[3] Bosio L, Johari G P and Teixeira J 1986 *Phys. Rev. Lett.* **56** 460
[4] Floriano M A, Whalley E, Svensson E C and Sears V F 1986 *Phys. Rev. Lett.* **57** 3062
[5] Bizid A, Bosio L, Defrain A and Oumezzine M 1987 *J. Chem. Phys.* **87** 2225
[6] Bellissent-Funel M C, Teixeira J and Bosio L 1987 *J. Chem. Phys.* **87** 2231
[7] Handa Y P, Mishima O and Whalley E 1986 *J. Chem. Phys.* **84** 2766
[8] Mishima O, Takemura K and Aoki K 1991 *Science* **254** 406
[9] Mishima O 1994 *J. Chem. Phys.* **100** 5910
[10] Mishima O 1996 *Nature* **384** 546
[11] Bellissent-Funel M-C 1998 *Europhys. Lett.* **42** 161
[12] Soper A K and Ricci M A 2000 *Phys. Rev. Lett.* **84** 2881
[13] Johari G P, Hallbrucker A and Mayer E 1987 *Nature* **330** 552
[14] Handa Y P and Klug D D 1988 *J. Phys. Chem.* **92** 3323
[15] Johari G P, Hallbrucker A and Mayer E 1991 *J. Chem. Phys.* **95** 6849
[16] Johari G P 1995 *J. Chem. Phys.* **102** 6224
[17] Velikov V, Borick S and Angell C A 2001 *Science* **294** 2335
[18] Klug D D, Mishima O and Whalley E 1987 *J. Chem. Phys.* **86** 5323
[19] Klug D D, Whalley E, Svensson E C, Rot J H and Sears V F 1991 *Phys. Rev.* B **44** 841
[20] Whalley E, Klug D D, Handa Y P, Svensson E C, Root J H and Sears V F 1991 *J. Mol. Struct.* **250** 337
[21] Svensson E C, Moontfrooij W and Klug D D 1994 *Physica* B **194–196** 409
[22] Li Jichen 1996 *J. Chem. Phys.* **105** 6733
[23] Kolesnikov A I, Sinitsyn V V, Ponyatovsky E G, Natkaniec I, Smirnov L S and Li L-C 1997 *J. Phys. Chem.* B **101** 6082
[24] Kolesnikov A I, Li J-C, Dong S, Bailey I F, Eccleston R S, Hahn W and Parker S F 1997 *Phys. Rev. Lett.* **79** 1869
[25] Kolesnikov A I, Li J-C, Parker S F, Eccleston R S and Loong C-K 1999 *Phys. Rev.* B **59** 3569
[26] Schober H, Koza M, Tölle A, Fujara F, Angell C A and Böhmer R 1998 *Physica* B **241–243** 897
[27] Tse J S, Klug D D, Tulk C A, Swainson I, Svensson E C, Loong C-K, Shpakov V, Belosludov V R, Belosludov R V and Kawazoe Y 1999 *Nature* **400** 647
[28] Klug D D, Tulk C A, Svensson E C and Loong C-L 1999 *Phys. Rev. Lett.* **83** 2584

[4] The authors wish to stress that [56, 57] have been published since the submission of the present publication.

[29] Schober H, Koza M M, Tölle A, Masciovecchio C, Sette F and Fujara F 2000 *Phys. Rev. Lett.* **85** 4100
[30] Mishima O and Stanley H E 1998 *Nature* **396** 329
[31] Stanley H E, Buldyrev S V, Canpolat M, Mishima O, Sadr-Lahijanin M R, Scala A and Starr F W 2000 *Phys. Chem. Chem. Phys.* **2000** 1551
[32] Debenedetti P G 1996 *Metastable Liquids—Concepts and Principles* (Princeton, NJ: Princeton University Press)
[33] Poole P H, Sciortino F, Essmann U and Stanley H E 1992 *Nature* **360** 324
[34] Speedy R J 1982 *J. Phys. Chem.* **86** 982
[35] Speedy R J 1982 *J. Phys. Chem.* **86** 3002
[36] Sastry S, Sciortino F and Stanley H E 1993 *J. Chem. Phys.* **98** 9863
[37] Stanley H E and Teixeira J 1980 *J. Chem. Phys.* **73** 3404
[38] Geiger A and Stanley H E 1982 *Phys. Rev. Lett.* **49** 1749
[39] Poole P H, Sciortino F, Grande T, Stanley H E and Angell C A 1994 *Phys. Rev. Lett.* **73** 1632
[40] Koza M, Schober H, Tölle A, Fujara F and Hansen T 1999 *Nature* **397** 660
[41] Koza M, Schober H, Hansen T, Tölle A and Fujara F 2000 *Phys. Rev. Lett.* **84** 4112
[42] 1994 *Guide to Neutron Research Facilities at the ILL* ILL
[43] Finney J L, Hallbrucker A, Kohl I, Soper A K and Bowron D T 2002 *Phys. Rev. Lett.* **88** 225503
[44] Doremus R H 1985 *Rates of Phase Transitions* (London: Academic)
[45] Primak W 1975 *The Compacted States of Vitreous Silica* (New York: Gordon and Breach)
[46] Karpov V G and Grimsditch M 1993 *Phys. Rev.* B **48** 6941
[47] Grimsditch M 1986 *Phys. Rev.* B **34** 4372
[48] Tsiok O B, Brashkin V V, Lyapin A G and Khvostantsev L G 1998 *Phys. Rev. Lett.* **80** 999
[49] Sciortino F and Tartaglia P 2001 *J. Phys.: Condens. Matter* **13** 9127
[50] Hage W, Hallbrucker A, Mayer E and Johari G P 1994 *J. Chem. Phys.* **100** 2743
[51] Hage W, Hallbrucker A, Mayer E and Johari G P 1995 *J. Chem. Phys.* **103** 545
[52] Angell C A, Poole P H and Shao J 1994 *Nuovo Cimento* D **16** 993
[53] Chen S-H and Teixeira J 1984 *Adv. Chem. Phys.* **64** 1
[54] Starr F W, Nielsen J K and Stanley H E 1999 *Phys. Rev. Lett.* **82** 2294
[55] Koza M M, Schober H, May R and Fujara F *Small Angle Neutron Scattering Results on the Transformation of HDA to LDA* paper in preparation
[56] Tulk C A, Benmore C J, Urquidi J, Klug D D, Neuefeind J, Tomberli B and Egelstaff P A 2002 *Science* **297** 1320
[57] Mishima O and Suzuki Y 2002 *Nature* **419** 599